17.6 Dielectrically Transduced Single-Ended to Differential MEMS Filter

Dana Weinstein, Hengky Chandrahalim, Lih Feng Cheow, Sunil A. Bhave

Cornell University, Ithaca, NY

Single-ended to differential micromechanical filters with large stop band rejection are ideal replacements for conventional SAW and FBAR filters [1,2] in sensor network transceivers and GSM and W-CDMA cell phones, which depend on differential signal paths. A differential output from the front-end filter eliminates the need for an off-chip balun in front-end radio design and increases filter linearity (Fig. 17.6.1). This paper reports on the design and performance of a single-ended input to differential output resonant electromechanical filter at 425MHz center frequency with 1MHz bandwidth (BW), 8dB insertion loss (IL), <5dB pass-band ripple, -50dB stop-band rejection, and -48dB common mode suppression (CMS), for a footprint of about $150\times150\mu m^2$.

Fully differential mechanical filters can be operated in single-ended to differential mode by providing only one of two input signals to actuate the filter. However, this method is not optimal since half of the drive electrode area is not utilized, resulting in a higher-than-necessary input motional impedance (R_X). The design presented here couples an intrinsically single-ended driving resonant mode to an inherently differential sensing resonant mode, thereby optimizing electrode area. The mechanical coupling between two different types of resonators enables us to achieve a CMS of -48dB, which is 20dB better than previously demonstrated bulk acoustic wave single-ended to differential filters [3, 4].

Lateral high-κ dielectric transduction increases both actuation force density and sensing capacitance, providing a κ^2 reduction in the motional impedance of the resonators over similar air-gap transduced devices [5]. These low R_X constituent resonators enable the design of low insertion loss filters. Furthermore, the resonators' high motional inductance (L_X), low motional capacitance (C_X), and high quality factor (Q) contribute to a small shape factor, making this filter ideal for channel-select narrow-band applications. Additionally, the dependence of resonant frequency on lateral dimensions allows for the fabrication of a switchable filter array covering a wide range of frequencies on a single chip. Each filter in the array can be switched on or off with the selective application of a DC polarization voltage to the device layer [6].

The filter, fabricated in the process described in [7], is comprised of two concentric resonators. An inner disk resonator (R_{disk} = 6.25μm) is dielectrically actuated to induce a radial contour mode [8]. Mechanical coupling from this inner disk to a concentric ring resonator drives a contour wine-glass mode in the outer ring (R_{in} = 32.6μm, R_{out} = 42.3μm) [9]. The coupling springs' stiffness is reduced by ensuring a flexure mode coupling using perpendicular arc segments (Fig. 17.6.2). The filter is suspended from the quasi-nodes of the wine glass ring. The anchor beams are frequency-matched to reflect back energy of the wine glass resonant mode but act as an energy sink for undesired ring modes.

The AC equivalent circuit of an electromechanical resonator is given by a series RLC circuit, where for a coupling constant $\eta \equiv V_{DC}\partial C/\partial x$, $R_X = b/\eta^2$, $C_X = \eta^2/K_{eff}$, and $L_X = M_{eff}/\eta^2$. The second-order electromechanical filter is modeled electrically by two resonator RLC circuits coupled through a capacitive T as illustrated in Fig. 17.6.3. When the resonators oscillate in phase, the current flowing through the shunt capacitor C_{CP} is minimized. When the resonators are out of phase, the current though the coupling shunt capacitor is at its maximum. In the mechanical domain, this corresponds to a minimal relative displacement of the coupling beam for in-phase resonance and a maximum beam displacement for out-of-phase resonance. In this model, feedthrough capacitance is negligible due to the large distance between drive and sense electrodes.

Figures 17.6.4 and 17.6.5 present PSPICE simulation results of the filter's AC equivalent circuit described above. For a 30nm thick hafnium dioxide dielectric layer, a numerical derivation of the radial disk mode yields R_{X1} = 590Ω, L_{X1} = 1.1mH, and C_{X1} = 127aF. The wine glass ring has R_{X2} = 93Ω, L_{X2} = 0.17mH, and C_{X2} = 805aF. Sweeping over coupling capacitance ($C_{CP} \sim k_{eff}^{-1}$) and load resistance R_Q, the filter BW and shape factor are presented. These contour plots provide graphical guidelines for designing the filter to meet a range of specifications.

The filter was tested on Cascade Microtech probe station, using an Agilent 8753ES network analyzer, a Minicircuits bias-T and 0/180° phase combiner. Figure 17.6.6 shows the 1MHz BW filter transmission response for a bias voltage of 5V and termination impedance of 4.8kΩ. An insertion loss of 8dB, shape factor of 1.16, stop band rejection of -50dB, and -48dB common mode suppression are observed. The CMS improved by 20dB over electrically coupled filters [3] due to the differential mechanical nature of the wine glass ring eigenmode. The filter has large insertion loss due to mismatch in the motional impedances of the constituent resonators. This can be improved by implementing a larger breathing mode ring for the inner resonator, increasing electrode area while maintaining the necessary symmetry.

The single-ended to differential filter prototype presented offers a channel-select switchable low-power electromechanical alternative for front-end RF receivers, eliminating the need for off-chip baluns and external RF switches. The high inductance and low capacitance of the dielectrically transduced resonators comprising the filter provide a small shape factor for narrow BW applications. Mechanical coupling greatly improves stop-band rejection, while the inherently differential mode shape of the wine glass ring provides excellent common mode suppression.

Acknowledgements:
The authors wish to thank NDSEG, Cornell Center for Nanoscale Systems, and Cornell Nanofabrication Facility.

References:
[1] R. Aigner, "High Performance RF-filters Suitable for Above IC Integration: Film Bulk-Acoustic- Resonators (FBAR) on Silicon," *Proc. Custom Integrated Circuits Conf.*, pp. 141-146, Feb., 2003.
[2] R. C. Ruby, et al, "High-Q FBAR Filters in a Wafer-Level Chip-Scale Package," *ISSCC Dig. Tech. Papers*, pp. 184-185, Feb., 2002.
[3] G. G. Fattinger, et al, "Single-to-Balanced Filters for Mobile Phones using Coupled Resonator BAW Technology," *Proc. Ultrasonics'04* , pp. 416-419, Aug., 2004.
[4] J. D. Larson, et al, "Film Acoustically-Coupled Transformer," *US Patent No. 2005/0093655 A1*, May 5, 2005.
[5] S. A. Bhave, et al, "Silicon Nitride-on-Silicon Bar Resonator using Internal Electrostatic Transduction," *Proc. Transducers'05*, pp. 2139- 2142, June, 2005.
[6] S. -S. Li, et al, "Self-Switching Vibrating Micromechanical Filter Bank," *to be published in Proc. IEEE Frequency Control Symposium*, Aug., 2005.
[7] H. Chandrahalim, et al, "Channel-Select Micromechanical Filters using High-K Dielectrically Transduced MEMS Resonators," *to be published in Proc. MEMS'06*, Jan., 2006.
[8] J. Clark, et al, "High-Q VHF Micromechanical Contour-Mode Disk Resonators," *Proc. IEDM'00*, pp. 493-496, Dec., 2000.
[9] Y. Xie, et al, "UHF Micromechanical Extensional Wine-Glass Mode Ring Resonators," *Proc. IEDM'03*, pp. 39.2.1 - 39.2.4, 2003.

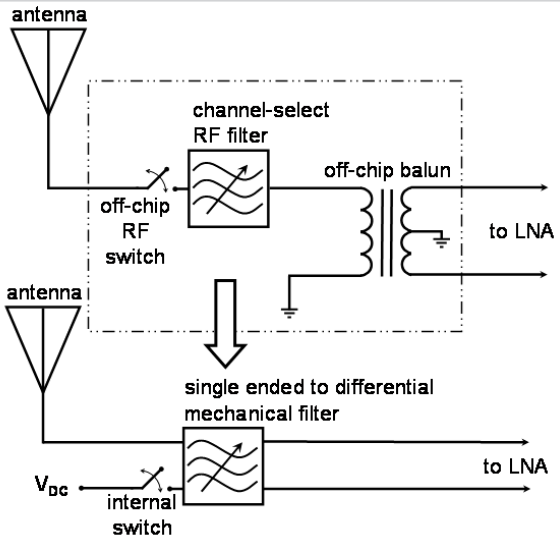

Figure 17.6.1: Front-end filter circuit for W-CDMA and GSM cell phones and sensor network radios.

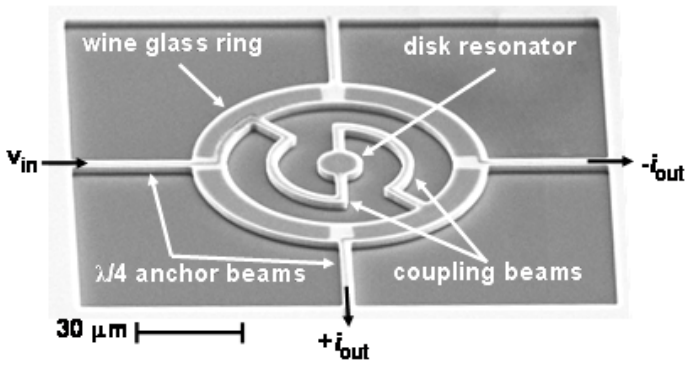

Figure 17.6.2: SEM of single-ended to differential filter.

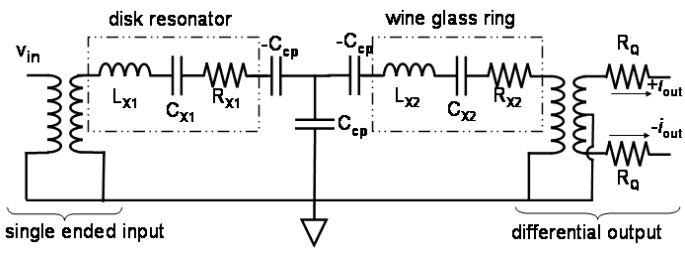

Figure 17.6.3: AC equivalent circuit of single-ended to differential filter.

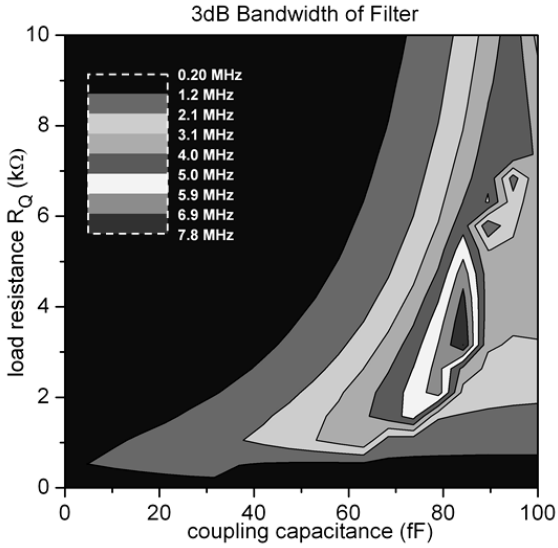

Figure 17.6.4: PSPICE analysis of filter 3dB bandwidth.

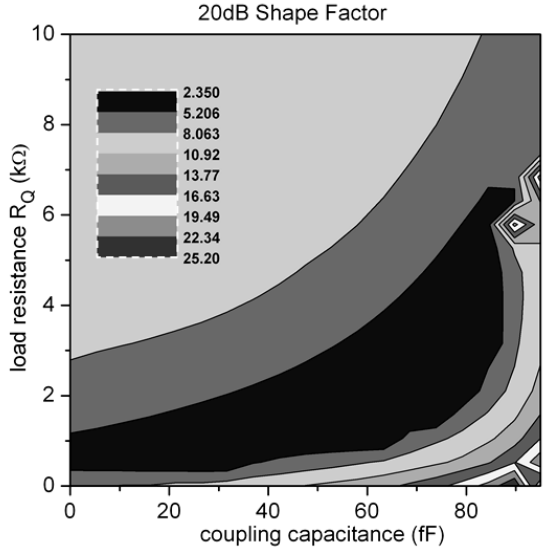

Figure 17.6.5: PSPICE analysis of filter 20dB shape factor.

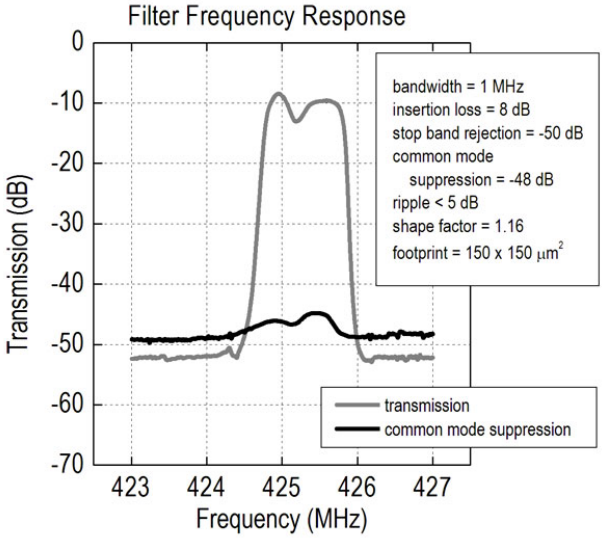

Figure 17.6.6: Filter frequency response.